AIMS Energy, 10(3): 412–433.
DOI: 10.3934/energy.2022021
Received: 03 February 2022
Revised: 20 April 2022
Accepted: 16 May 2022
Published: 25 May 2022

http://www.aimspress.com/journal/energy

Research article

Experimental investigation and exergy and energy analysis of a forced convection solar fish dryer integrated with thermal energy storage

Dessie Tadele Embiale, Dawit Gudeta Gunjo, Chandraprabu Venkatachalam and Mohanram Parthiban*

Department of Mechanical Engineering, Adama Science and Technology University, Adama, Ethiopia.

* **Correspondence:** Email: lillymohan@yahoo.com; Tel: +251966684023.

Abstract: Drying is an effective means of reducing post-harvest losses which increases the shelf life of products by reducing their moisture content to a safe storage level. An indirect mode forced convection solar dryer integrated with thermal energy storage was designed, developed and experimentally tested by drying fish. The components of the dryer are a double pass solar air heater, a paraffin wax-based shell and tube for latent heat thermal energy storage, a drying chamber and a blower. A maximum temperature of 69 ℃ was obtained at the outlet of the solar air heater, and the energy and exergy efficiencies were 25% and 1.5%, respectively. The latent heat storage reduces the fluctuations in the outlet temperature of the solar air heater and extends the drying process for two extra hours per day. The average energy and exergy efficiencies of the energy storage were 41.9% and 15.6%, respectively, whereas average energy and exergy efficiencies of the drying chamber were 35% and 52%, respectively. Moreover, 5 kg of fresh fish was effectively dried in the dryer within 21 hrs, reducing the moisture content of the fish from 75% to 12.5% by removing 3.57 kg of moisture. The specific energy consumption of the dryer was 7.3 kWh per kilogram of moisture, and the power consumed by the blower was 0.6 kWh per kilogram of moisture, which is 8.3% of the total energy consumption. The remaining 91.7% of the energy is harvested from the sun, and the overall efficiency of the drying system is 9.4%.

Keywords: drying; thermal energy storage; fish; paraffin wax; exergy efficiency

Nomenclature: LHS: Latent heat storage; PCM: Phase change material; SAH: Solar air heater; A: Area (m^2); I: Solar radiation (W/m^2); C_p: Specific heat ($kJ/(kg \cdot K)$); E: Energy (J); L_f: Latent heat of

fusion (KJ/kg); M: Moisture content (%); Q: Heat (W); T: Temperature (°C); U: Overall heat loss coefficient (W/m^2. K); Z: Height (m); g: Gravity (m/s^2); h: Enthalpy (kJ/kg.); m: Mass (kg); t_d: drying time (s); w.b: wet basis; hrs: hours

Subscripts: dc: Drying chamber; ch: Charging; dich: Discharging; ES: Energy storage; amb: Ambient; i: inlet; o: outlet; a: air

1. Introduction

Drying is an effective means of reducing post-harvest losses which increases the shelf life of products by reducing the moisture content to a safe storage level, and it has been practiced for a long time. The purpose of drying is removing water from the food so that the growth of microorganisms (bacteria, yeasts and molds) can be inhibited. According to food scientists, reducing the moisture content of food between 10% and 20% prevents microorganisms from spoiling the food, and most of the nutritional value and flavor can also be preserved. Products that can be preserved by drying include agricultural products (cereals), medical plants, fruits, vegetables, fish and meat [1].

Fresh fish rapidly deteriorate without external contamination in less than 24 hours. The reason behind this is that fish harvesting occurs with an average moisture content of 75% (wet basis (w.b.)) [2]. Fish can be preserved using several techniques (including traditional preservation techniques), such as freezing, cold storage (chilling), dehydration (salting, drying and smoking) and use of chemical treatments [3]. Open sun drying is the most widespread method of drying fish and has been practiced since ancient times. However, despite the fact that it is simple and inexpensive, traditional open sun drying has disadvantages. It needs a large area exposed to direct sunlight, and there is loss of dried products due to rats, cats, dogs, birds and infestation with insects. Wind, rain, moisture and dust spoil the product, and fish drying with unstable moisture content in a slow drying process creates favorable conditions for microorganism proliferation, which becomes a source of food poisoning. Additionally, exposing products like fish to direct sunlight destroys light-sensitive nutrients present in fish [4]. Hence, to control this problem, other hygienic and environmentally friendly drying technologies must be developed and adopted for the drying of fish with best quality. Nowadays, solar drying technologies are getting popular. In solar drying, products are dried at an elevated temperature using special devices called solar dryers. However, the intermittent nature of and uncertainty in the availability of solar energy are the main drawbacks in solar drying. These drawbacks can be eliminated with the integration of auxiliary heating devices like biomass backup heaters, electric heaters, wood stoves, liquid or gas fuel burners or thermal energy storage units, which include sensible heat storages and latent heat storages. In sensible heat storage systems, the energy is stored by changing the temperature of a storage material like concrete, sand-rock minerals, ferroalloy materials, bricks, etc. Meanwhile, in latent heat storages, the heat transfer occurs when substances like salt nitrates, paraffin wax, etc. change their phases from solid to liquid and vice versa. Latent heat storage systems store higher amounts of energy per unit of storage material compared to sensible heat storage systems [5].

A lot of research has been done on solar drying of products like fruits, vegetables, agricultural products (cereals), medical plants, fish and meat. The products are dried in solar dryers like direct solar dryers, in which the products are exposed to direct sunlight, and indirect solar dryers, in which the products are placed inside the drying chamber, and hot air is supplied from the solar air heater. A solar tent dryer was developed to reduce fish post-harvest losses [6]. Locally available materials like wood, white and black plastic, nail, rope and wire mesh were used to construct the dryer, and a total moisture

loss of 60% was obtained in three days. A solar drying model for selected Cambodian fish species was developed and compared it with the electric oven dryer [7]. The results showed that the average drying temperature and relative humidity in the solar dryer were 55.6 ℃ and 19.9%, respectively. The overall efficiency of the solar dryer, corresponding to 15% of final product moisture content, was 12.37%. It was also concluded that the drying rates were higher in the solar drying process compared to the control drying in an electric oven. Solar dryers integrated with sensible heat storage materials to enhance their performance have also been studied. The performance of a natural convection solar tunnel dryer integrated with a rock bed as a sensible heat storage material was tested for drying copra [8]. The results showed that the moisture content of the copra was reduced from 52% (w.b.) to 7.1% (w.b.) in 54 h with storage, in 60 h without heat storage material and in 153 h in open sun drying. The average thermal efficiency of the dryer was 15% and was increased by 2% to 3% using the storage. An experimental investigation of a natural convection solar greenhouse dryer integrated with sensible heat storage materials for drying coconuts was conducted [9]. The results showed that the moisture content of coconuts was reduced from 52% (w.b.) to 7% (w.b.) in 78 h, 66 h and 53 h using concrete, sand and rock bed, respectively, for savings of 55%, 62% and 69%, respectively, compared to open sun drying, which took 174 h. The dryer efficiencies were 9.5%, 11% and 11.65% using concrete, sand and rock bed, respectively. Performance of a forced convection solar dryer with granite stone as a sensible heat storage material was studied [10]. Air flow rates between 0.016 kg/s and 0.08 kg/s were used for experimentation. The temperature distribution along the air heater was discussed, and the results showed that the solar air heater gave an outlet temperature of 10 ℃ to 25 ℃ more than the ambient.

Integrating latent heat thermal energy storage systems with solar dryers is getting more popular nowadays due to their high heat storing capacities compared to sensible heat storage materials. Previous works on solar drying systems which use phase change materials (PCMs) for energy storage were reviewed [11]. It was concluded that recent studies focused on PCMs as energy storage media because of their higher thermal energy storage densities compared with sensible heat storage materials. It was also concluded that implementing PCMs in solar dryers reduces heat losses and improves efficiency. An indirect type of solar fish dryer with PCM was experimentally analyzed [5]. For experimentation, two different PCMs, paraffin wax C23–24 (45–48 ℃) and paraffin wax C31–33 (68–70 ℃) were used. The results showed that, out of the total available heat, 40% of the heat was utilized, 60% was found to be exhausted unutilized, and the use of PCM was found to be an excellent solution to accumulate this heat. PCM-1 maintains an average temperature higher than the average temperature of the dryer without PCM, and the drying period was reduced by up to approximately 80% comparted to the traditional method and by 20% compared to the solar dryer method. PCM-2 was also tested for load condition, and the average temperature maintained was 36.5 ℃. It was stated that, due to the temperature range of the drying process, PCM-2 was not suitable for this application. A natural convection solar dryer integrated with paraffin wax based latent heat storage was designed and developed [12]. Initial measurements of temperature at the inlet of, at the outlet of, at the back of and below the solar panel with free natural circulation of air were carried out daily. The results showed that the continuous drying of agricultural/food products at a steady and moderate temperature of 40–75 ℃ can be possible. Experimental investigation of an indirect mode forced convection solar dryer integrated with latent heat storage for drying medical plants was carried out [13]. A no-load test of the dryer was performed with and without PCM at mass flow rates of 0.0664 kg/s to 0.2182 kg/s. The results showed that using the PCM gave a drying air temperature 2.5 ℃ to 7.5 ℃ higher than ambient temperature after sunset for at least 5 hours. After implementing the PCM, the final moisture content

was achieved in 12–18 h. A solar dryer integrated with PCM was developed and tested experimentally by drying mushrooms [14]. The results showed that a temperature rise of 20 ℃ above the ambient was supplied by the accumulator for 2 h, and 40–70% of electrical energy was saved. The thermal efficiencies of the solar air heater and the accumulator were in the ranges of 22% to 67% and 10% to 21%, respectively. A direct type solar dryer integrated with a paraffin wax based latent heat storage (LHS) system was developed by [15]. The results showed that a drying temperature 6 ℃ higher than the ambient was supplied by the energy storage system for about 5 h to 6 h after sunset. A solar dryer integrated with a thermal energy storage system with and exhaust air recirculation system was developed [16]. The results showed that, without recirculation of the exhaust air, the exergy efficiency was in the range of 5% to 55% in the first 3 h of the drying period. Thereafter, the exhaust air was re-circulated, and the exergy efficiency was 67% to 88%. A natural convection mode solar dryer integrated with a paraffin wax based LHS system was studied [17]. The dryer was tested under both full-load (with ginger) and no-load conditions. The results from the test showed that the moisture content of ginger was reduced from 74% to 3% in 24 h, and daily drying efficiency was 12.4%. Collector efficiency during no-load testing was in the range of 53% to 96%, and during full-load testing it was in the range of 40% to 55%.

Photovoltaic assisted mixed mode greenhouse solar dryer integrated with thermal energy storage using paraffin wax and an exhaust air recirculation system was developed [18]. The dryer was developed to dry bitter gourd, and two DC fans and photovoltaic panels were used. The performance of the dryer was tested with and without the thermal energy storage system, and it was reported that the integration of the thermal storage system improved the performance of the dryer. The thermal efficiencies of the dryer were 18.6% and 10.8% with and without the thermal energy storage system, respectively. Economic analysis was also performed, and the payback period of the dryer was 1.91 years. The performance of a mixed mode solar greenhouse dryer with and without a thermal energy storage system for drying pepper was also tested [19]. Paraffin wax was used as a PCM, and it was reported that the air temperature inside the solar greenhouse dryer with PCM was higher than in the dryer without PCM by 7.5 ℃. It was also reported that there was a 95% moisture content reduction in 30 hours, 55 hours and 75 hours for the dryer with PCM, the dryer without PCM and open sun drying, respectively. Experimental investigation of a natural convection indirect mode solar dryer with PCM for drying of banana slices was presented [20]. A paraffin wax layer with a melting temperature of 48 ℃ was placed in the solar air heater (SAH) between the absorber and the base plates. Two equally spaced trays were used in the drying chamber, and banana slices were dried from 73.2% (w.b.) to 20% (w.b.) in 18 h. The thermal efficiency of the dryer was 2.9%. It was also reported that adding the PCM in the SAH helps the dryer to effectively operate for 5 h per day after sunset. Experimental investigation to test the performance of a solar dryer with paraffin wax as a PCM packed on its floor was presented [21]. Four crop samples (guava, banana, coconut and ladies' fingers) were tested in the dryer with and without the PCM, and it was reported that installing the PCM in the dryer reduced the drying time of all products by about 3–4 hours, thereby reducing the drying time of the crops per day. It was also reported that the color, fragrance and quality of the products dried in the solar dryer were better than those of the sun-dried products. Performance of a solar dryer integrated with thermal energy storage using an evacuated tube heat pipe as a collector to dry agricultural products like tomatoes and carrots was designed and studied [22]. Therminol 55 was used as for thermal energy storage, and a maximum outlet air temperature of 118 ℃ was achieved in the collector. The average energy and exergy efficiencies of the collector varied in the ranges of 10% to 30% and 1.9% to 5.6%, respectively,

and the payback period of the dryer was 2.6 years. Performance of a solar dryer integrated with thermal energy storage by drying blood fruit was also studied [23]. It was reported that the integration of the energy storage increases the drying time by 19% at off-sunshine hours. The quality of the dried products was also retained, and the payback period of the dryer was 1.23 years. The performance of a solar dryer with a tube type absorber packed with aluminum wool to enhance the performance was studied [24]. The results showed that the performance was improved by using the aluminum wool in the tube, and the drying time was also reduced by 30%. Performance of a greenhouse dryer was studied by integrating a solar absorber north wall coated with graphene nanoplatelet-embedded black paint to enhance its performance [25]. It was reported that the enhancement methods (north wall and nano-enhanced north wall) reduced the drying time by 75 mins and 90 mins, respectively, and the exergy efficiencies were 4.67% and 5.38%, respectively. A vertical hybrid photovoltaic thermal solar dryer integrated with fins was developed and analyzed [26]. It was reported that the thermal efficiencies of the collector were in the ranges of 47.46% to 54.8% and 50.25% to 58.16% for finless and finned collectors, respectively. The average exergy efficiencies of the drying chamber were 41.85%, 44.17% and 52.01% for the finless collector and 43.04%, 49.18% and 56.11% for the finned collector. Sustainability analysis of a photovoltaic driven square-spiral finned quadruple-flow solar collector assisted dryer was performed [27]. The results showed that the average exergy efficiency of the collector was between 73.27% and 78.19%, and the sustainability index was between 1.93 and 2.73.

Most of the previous works on solar dryers focus on the drying of agricultural products, fruits, vegetables and medical plants. There are also very few attempts on drying of fish, but these dryers solely work in the time when sunlight is available. Also, in the existing methods, thermal energy storages are placed either at the bottom of the absorber plate or in the drying chamber. Placing the thermal energy storage at these two sections of the dryers has some disadvantages, like the loss of heat from the storage to the sides and top of the absorber and the drying chamber. To minimize this heat loss, a separate system can be used. Studies on thermal energy storage systems show that shell and tube LHS systems with horizontal orientation have better performances and faster melting rates of the PCMs compared to other LHS systems like vertically oriented shell and tube LHS and rectangular type LHS systems [28–30]. Hence, this type of storage can be used in solar dryers and can be placed between the SAH and the drying chamber with proper insulation to minimize heat loss from the shell of the storage. Studies on exergy and energy analysis of solar dryers integrated with shell and tube type LHS systems are also limited. Therefore, this study focuses on exergy and energy analysis of a solar fish dryer integrated with thermal energy storage with a separate arrangement of the dryer and thermal energy storage system. Since temperature control is one of the advantages of thermal energy storage systems, the separate arrangement can provide better temperature control of the hot air entering into the drying chamber.

2. Materials and methods

A forced convection type solar dryer integrated with a thermal energy storage system was manufactured and assembled at a local site (Adama). Paraffin wax was used as a latent heat thermal energy storage material. Exergy and energy analysis was used to evaluate the performances of the dryer and each component of the dryer.

Table 1. Thermophysical properties of the PCM [31].

PCM	Melting point (℃)	Heat of fusion (kJ/kg)	Thermal conductivity (W/(m·K))	Density (kg/m^3)	Specific heat (kJ/(kg·K))
Paraffin wax	58–60	189	0.22	918	2.384

2.1. Experimental setup

An indirect mode solar dryer integrated with a PCM was designed and developed for experimentation as shown in Figure 1. The components of the dryer are a 2.06 m^2 double pass SAH, a thermal energy storage unit filled with 16 kg of paraffin wax with a melting temperature of 58 ℃, a 1 m × 0.9 m × 1 m drying chamber and a 0.1 kW and 1300 rpm blower. The energy storage is a shell and tube type LHS with a shell diameter of 0.2 m and 1 m length and with 5 steel tubes with a diameter of 0.016 m. The trays of the drying chamber were made from wire mesh, and a total of 5 trays were used.

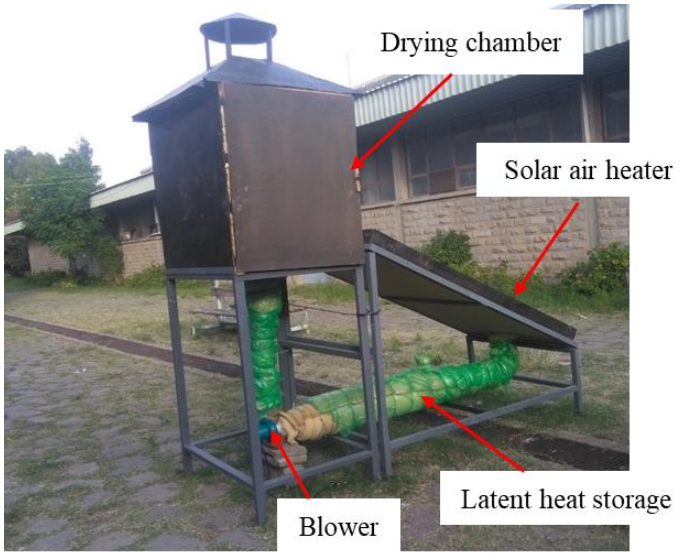

Figure 1. Experimental setup.

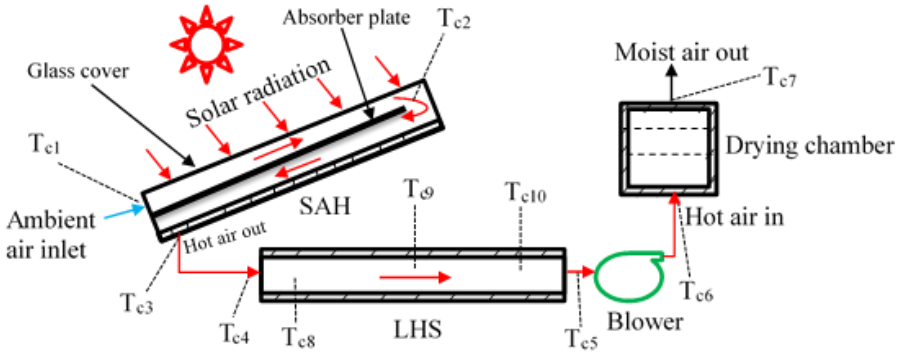

Figure 2. Schematic layout of the solar dryer (Tc-thermocouple).

In this drying system, a double pass SAH is used to get the desired drying air temperature. Air at ambient temperature is passed through the SAH, where it is heated up by trapping the solar energy incident on its surface. The air first passes between the glass cover and the absorber plate and then passes under the absorber plate. The air exiting from the SAH passes through the tubes of the shell and tube LHS located between the SAH and the drying chamber. When the temperature of the air coming out of the SAH is higher than the temperature of the PCM, the heat is transferred from the air to the PCM (charging period). In contrast, when the temperature of the air coming out of the SAH is lower than the temperature of the PCM, the accumulated thermal energy is released from the PCM (discharging period), resulting in an increase in the temperature of the air. The air leaving the LHS is then drawn into the drying chamber with the blower. The hot air flows over the product on the drying trays and escapes to the atmosphere after removing the moisture from the products.

2.2. Experimental procedure

A K-type thermocouple was used to measure temperature at different locations of the dryer. Two thermocouples were placed at the inlet and outlet of the SAH, and another thermocouple was placed at the outlet of the first fluid pass to measure the temperature of the air. Three thermocouples were placed inside the thermal energy storage to measure the temperature of the PCM, which determines whether the PCM is completely melted or not. Another two thermocouples were placed at the inlet and outlet of the LHS to measure the temperatures of the incoming and leaving air, i.e., to and from the storage. Two thermocouples were placed at the inlet and outlet of the drying chamber to measure the temperature at each location. A no-load test was done to check whether the outlet air temperatures of the SAH and the energy storage were in the desired ranges for the drying application. During the load test, the trays of the drying chamber were loaded with 5 kg of fresh fish, and the inlet and outlet temperatures of the drying chamber were recorded to evaluate its performance. Four samples were taken from four different locations and weighed at a three-hour interval to determine the moisture loss from the fish.

Table 2. Specifications of the measuring instruments.

Measuring instrument	Brand	Serial number	Range	Power supply	Weight (approx.)	Accuracy
Thermocouple	Hti	HT-9815	0–800 ℃	9 V	250 g	±2 ℃
Digital balance	CAS	SW-20	50 g–10 kg	-	5 kg	±0.5 g

2.3. Sample preparation

Prior to experimentation, the following procedure was used to prepare the fish for drying.

(1) The raw fresh fish was cleaned with clean and fresh water.
(2) The gills and internal organs were removed by splitting, and then it was washed thoroughly and drained.
(3) A salt solution was prepared (60 g salt dissolved in 1 L of water), and the fish was soaked in it for one hour.
(4) The salted fish was drained and arranged on the trays without placing the fish on top of each other.

To determine the initial moisture content of the fish, 0.1 kg of fish was dried in an oven at a

temperature of 105 ℃ for 24 hours. The final mass of the oven dried fish was weighed to determine the moisture content, and it was found to be 75.1%.

2.4. Energy and exergy analysis

Energy and exergy analysis helps to evaluate the performance of a system in terms of energy and exergy efficiencies.

2.4.1. Energy analysis

The general mass and energy conservation equations for the steady flow open system can be expressed as follows [32]:

$$\text{Mass balance: } \sum \dot{m}_i = \sum \dot{m}_o \tag{1}$$

$$\text{Energy balance: } \dot{Q} - \dot{W} = \sum \dot{m}_o \left(h_o + \frac{{v_o}^2}{2} + Z_o g\right) - \sum \dot{m}_i \left(h_i + \frac{{v_i}^2}{2} + Z_i g\right) \tag{2}$$

2.4.1.1. Energy analysis of the solar air heater

The mass and energy conservation equations for the SAH can be expressed as follows [33]:

$$\dot{m}_o = \dot{m}_i = \dot{m}_a \tag{3}$$

$$\dot{Q}_{inSAH} - \dot{Q}_{lSAH} = \dot{m}_o(h_o - h_i) \tag{4}$$

where $\dot{Q}_{inSAH}$ is the rate of heat input to the SAH:

$$\dot{Q}_{inSAH} = \alpha_a \tau_c I A_{SAH}. \tag{5}$$

The right-hand term of Eq (4) is the rate of useful heat gained by the SAH [34]:

$$\dot{Q}_{uSAH} = \dot{m}_a C_{pa}(T_{oSAH} - T_{iSAH}) \tag{6}$$

Energy efficiency is the ratio of the useful heat gained to the absorbed solar energy [33]:

$$\eta_{SAH} = \frac{\dot{m}_a C_{pa}(T_{oSAH} - T_{iSAH})}{\alpha_a \tau_c I A_{SAH}} \tag{7}$$

2.4.1.2. Energy analysis of the thermal energy storage

The instantaneous energy input to the energy storage and instantaneous energy recovered from the energy storage during the charging and discharging processes are determined as follows [35]:

$$\dot{Q}_{ich} = \dot{m}_a C_{pa}(T_{iES} - T_{oES}) \tag{8}$$

$$\dot{Q}_{odich} = \dot{m}_a C_{pa}(T_{oES} - T_{iES}) \tag{9}$$

2.4.1.3. Energy analysis of the drying chamber

During the dehumidification process in the drying chamber, the heat used is estimated as follows [36]:

$$\dot{Q}_{dc} = \dot{m}_a C_{pa}(T_{idc} - T_{odc}) \tag{10}$$

The thermal efficiency of the drying chamber is the ratio of the actual temperature drop to the maximum possible temperature drop of the drying air [37].

$$\eta_{dc} = \frac{(T_{idc} - T_{odc})}{(T_{idc} - T_{amb})} \tag{11}$$

2.4.2. Exergy analysis

Exergy analysis provides an alternative means of assessing and comparing processes and systems and yields efficiencies which provide a true measure of how nearly the performance of an actual system approaches the ideal [35].

The general form of a steady flow exergy equation is expressed as follows [37]:

$$\dot{E}x = \dot{m}_a C_{pa}\left(T - T_{amb} - T_{amb}\ln\frac{T}{T_{amb}}\right) \tag{12}$$

2.4.2.1. Exergy analysis of the solar air heater

Exergy input to the SAH is as follows [38]:

$$\dot{E}x_{inSAH} = \left[1 - \frac{T_{amb}}{T_s}\right]\dot{Q}_{inSAH} \tag{13}$$

where T_s is apparent sun temperature, assumed to be 4500 K (75 % of black body temperature of the sun). The exergy received by the air is as follows:

$$\dot{E}x_{rSAH} = \dot{m}_a C_{pa}\left[(T_{oSAH} - T_{iSAH}) - T_{amb}\ln\left(\frac{T_{oSAH}}{T_{iSAH}}\right)\right] \tag{14}$$

Exergy efficiency:

$$\eta_{ExSAH} = \frac{\dot{m}_a C_{pa}\left[(T_{oSAH} - T_{iSAH}) - T_{amb}\ln\left(\frac{T_{oSAH}}{T_{iSAH}}\right)\right]}{\left[1 - \frac{T_{amb}}{T_s}\right]\dot{Q}_{inSAH}} \tag{15}$$

2.4.2.2. Exergy analysis of the energy storage

The instantaneous exergy input to the energy storage and instantaneous exergy recovered from the energy storage during the charging and discharging processes are expressed as follows [35]:

$$\dot{E}x_{ich} = \dot{m}_a C_{pa}\left[(T_{iES} - T_{oES}) - T_{amb}\ln\left(\frac{T_{iES}}{T_{oES}}\right)\right] \tag{16}$$

$$\dot{E}x_{odich} = \dot{m}_a C_{pa}\left[(T_{oES} - T_{iES}) - T_{amb}\ln\left(\frac{T_{oES}}{T_{iES}}\right)\right] \quad (17)$$

2.4.2.3. Exergy analysis of the drying chamber

The exergy inflow and outflow to and from the drying chamber are determined as follows [37]:

$$\dot{E}x_{idc} = \dot{m}_a C_{pa}\left[(T_{idc} - T_{amb}) - T_{amb}\ln\left(\frac{T_{idc}}{T_{amb}}\right)\right] \quad (18)$$

$$\dot{E}x_{odc} = \dot{m}_a C_{pa}\left[(T_{odc} - T_{amb}) - T_{amb}\ln\left(\frac{T_{odc}}{T_{amb}}\right)\right] \quad (19)$$

The exergy efficiency is as follows:

$$\eta_{Exdc} = \frac{\dot{E}x_{odc}}{\dot{E}x_{idc}} \quad (20)$$

2.5. Performance of the drying system

The performance of the PCM integrated solar drying system can be evaluated in terms of specific energy consumption and overall drying efficiency of the system [37].

Specific energy consumption is the ratio of the total energy input to the total moisture removal from the product.

$$SEC = \frac{P_t}{m_v} \quad (21)$$

where P_t is the total energy input, which is the sum of the solar energy incident on the surface of the SAH and the electrical energy consumed by the blower:

$$P_t = (A_{SAH} I + P_b) t_d \quad (22)$$

The overall thermal efficiency of the drying system is the ratio of the energy required to evaporate the moisture from the product to the total energy input into the drying system.

$$\eta_{ds} = \frac{m_v h_{fg}}{P_t} \quad (23)$$

3. Results and discussion

3.1. Inlet and outlet temperature variations of the SAH

The variations of ambient air temperature and outlet air temperature of the SAH with time for the five days are presented in Figure 3. It is observed that the outlet temperature of the SAH increased with increasing solar radiation intensity. This was due to the fact that, as the solar radiation intensity increases, the amount of heat absorbed by the SAH increases, and the temperature of the absorber plate rises. The air passing through the SAH then absorbs more heat from the absorber plate, and its

temperature also rises. The absorber plate temperature starts to decrease as the solar radiation intensity, decreases resulting in a decrease in temperature of the air passing through it. The outlet temperature of the SAH starts increasing and becomes maximum between 12:00 and 14:30, and it starts to decrease when the solar radiation decreases and becomes almost equal to the ambient at 18:30. The maximum outlet temperature recorded was 69.5 ℃ at 13:30, and the minimum was 35 ℃, recorded at 9:00. The ambient temperature varies between 25 ℃ and 32 ℃ each day. Fluctuations are observed during the first, third and fifth (19th, 24th and 26th) days of the experiment due to cloud covers.

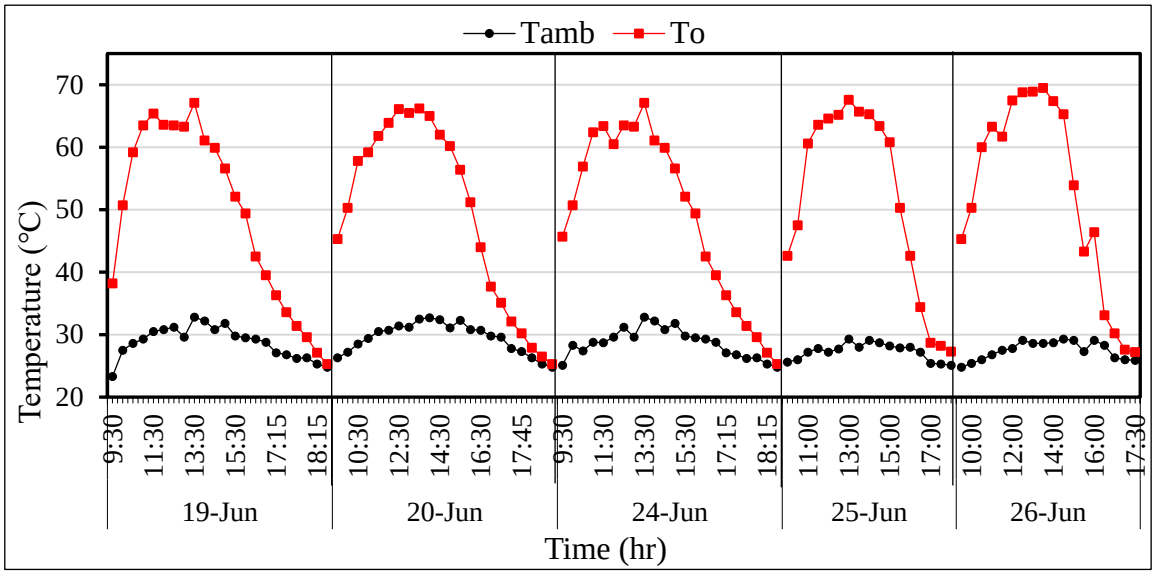

Figure 3. Variations of inlet and outlet temperatures of the SAH with time.

3.2. Variation of thermal and exergy efficiency of the solar air heater

The variations of the thermal and exergy efficiencies of the solar air heater with time are illustrated in Figure 4. The thermal efficiency of the SAH increased with increasing solar radiation intensity and decreased when the intensity became low. When the solar radiation intensity is high, the SAH absorbs more heat, and this heat is transferred to the air, resulting in the rise of its temperature and thereby increasing the efficiency of the SAH. When the intensity falls, the amount of heat absorbed by the SAH decreases, the air temperature decreases with it, and the efficiency decreases. The maximum thermal efficiency of the SAH was 35%, and the minimum was 10%, from 9:30 to 16:30. The average thermal efficiency of the SAH was 25%. References [39] and [40] reported similar results (26% and 29%) of average thermal efficiencies of a double pass SAH. Similar to the thermal efficiency, the exergy efficiency of the SAH also increased and decreased as the solar radiation intensity increased and decreased, respectively. The exergy efficiency increased as the outlet temperature increased, with maximum values obtained around 13:00. Maximum exergy efficiencies were found in the last two days of the experiment due to the high outlet temperature and low inlet temperature of the SAH compared to the first two days. The maximum exergy efficiency of the SAH was 2%, obtained at 13:00, and the minimum was 0.4%, obtained at 9:30. The average exergy efficiency of the SAH was 1.5%. Similar results of exergy efficiency of SAHs was reported by [41].

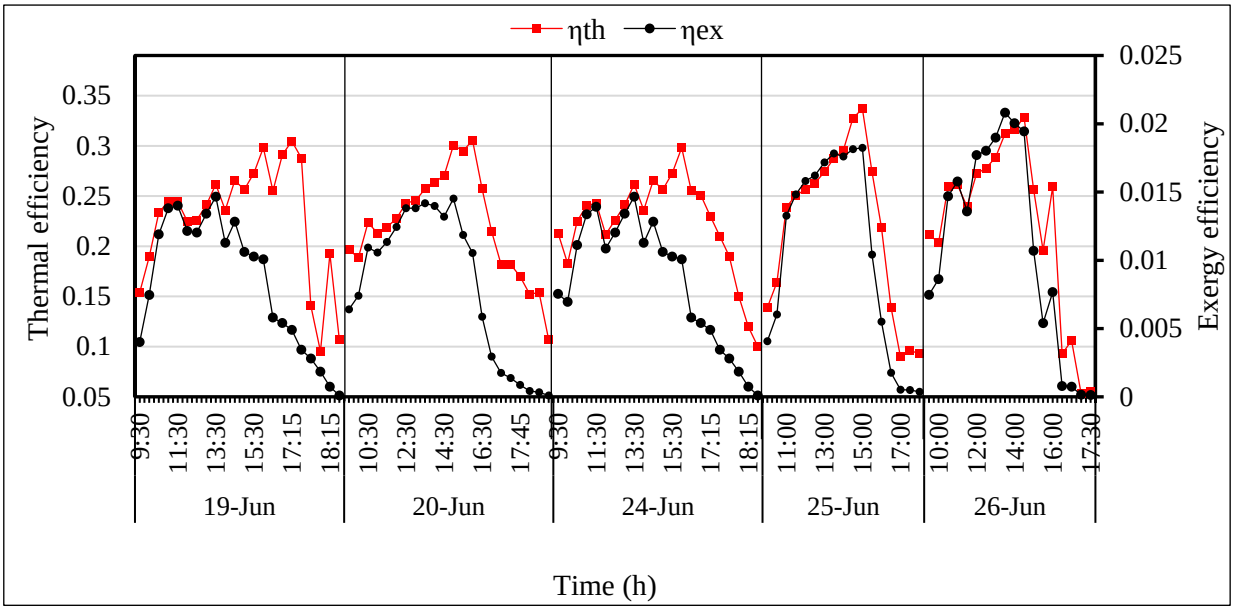

Figure 4. Variations of thermal and exergy efficiencies of the SAH with time.

3.3. Variations of inlet and outlet temperatures of the energy storage

Figure 5 shows the variations of the inlet and outlet air temperatures of the thermal energy storage during the charging and discharging processes. It is observed that the inlet air temperature varied between 35 ℃ and 70 ℃, whereas the outlet temperature varied between 30 ℃ and 60 ℃. During the charging period, the inlet temperature of the storage is higher than the outlet, since heat is transferred from the air to the PCM. In contrast, during the discharging period, heat is transferred from the PCM to the air, and the outlet temperature of the storage is higher than that of the inlet. The inlet temperature of the storage varied with the changes in solar intensity. It started increasing and became maximum between 12:00 and 14:30, and it started decreasing and became almost equal to the ambient at 18:30. However, the outlet air temperature remained 5 ℃ to 10 ℃ higher than the inlet after 16:30. Charging started at 09:30 and completed around 14:30, and discharging started around 15:30, when the inlet air temperature was lower than the storage temperature. During the charging process, the highest drop in air temperature, of 12 ℃, between the inlet and outlet of the storage was observed, and during the discharging process, a rise in air temperature of 10 ℃ was observed. When the temperature of the air does not change while passing through the energy storage, the PCM is assumed to be completely melted. The point where the inlet and outlet temperatures of the storage intersect indicates the end of the charging period and the beginning of the discharging period. Fluctuations in the inlet temperature of the storage are observed in the first, third and fifth days of the experiment due to fluctuations in solar radiation, but the energy storage diminishes these fluctuations and supplies the air at a constant temperature to the drying chamber.

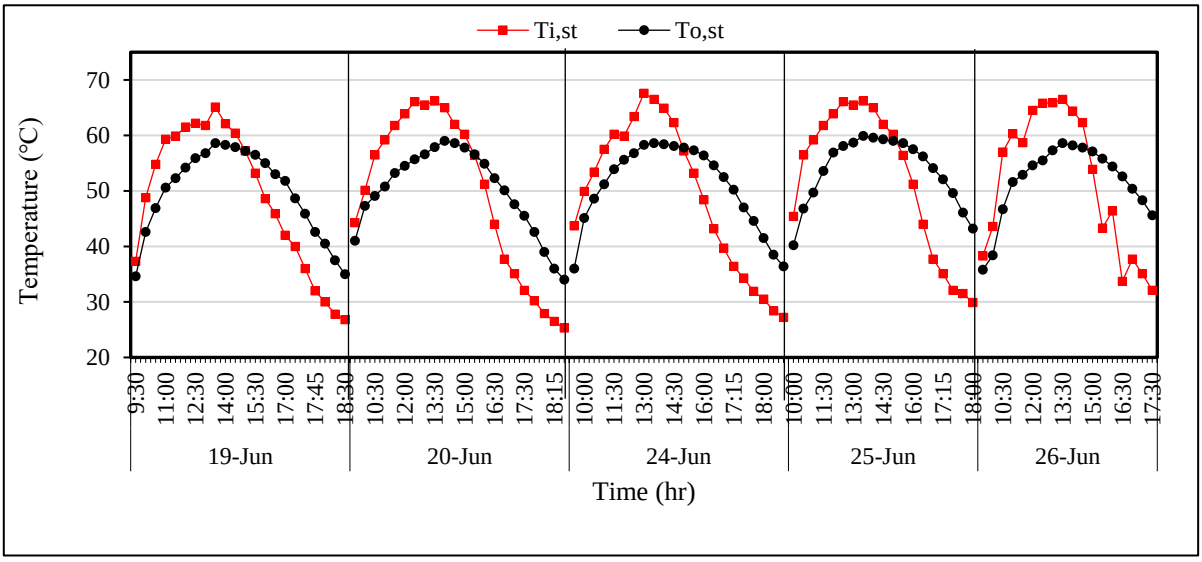

Figure 5. Inlet and outlet temperature variations of the energy storage.

3.4. Heat input/recovered during the charging and discharging processes

The instantaneous heat input and heat recovered during the charging and discharging processes are presented in Figure 6. The positive and negative values on the secondary y-axis represent the heat input and heat recovered by the air, respectively. The heat input started increasing with the increase in the inlet air temperature and became maximum around 13:00. It started to decrease as the inlet temperature decreased and became zero when the inlet and outlet air temperatures became equal (end of charging period). Heat recovery started (beginning of discharging period) when the inlet air temperature became less than the temperature of the PCM. The average instantaneous heat input during the charging process of the energy storage varied between 106 W and 125 W, and the heat recovered by the air during the discharging process varied between 83 W and 110 W.

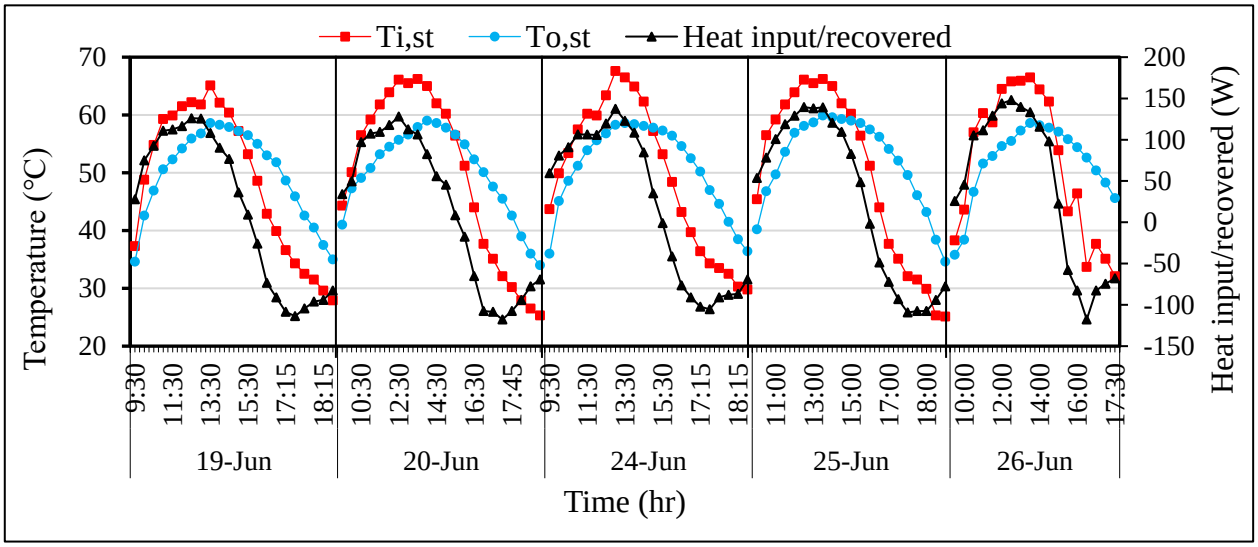

Figure 6. Heat input/recovered by the air during the charging and discharging processes.

3.5. Exergy input/recovered during the charging and discharging processes

Figure 7 represents the instantaneous exergy input and exergy recovered during the charging and discharging processes of the energy storage, shown as positive and negative on the secondary y-axis, respectively. The exergy input first increased with the increase in inlet temperature. It started to decrease when the inlet temperature decreased and became zero when the inlet and outlet temperatures became equal (charging period). During the discharging period, the exergy recovered increased with the increase in heat recovered and started decreasing when the temperature of the PCM becames low. The average instantaneous exergy input during the charging process varied between 6.3 W and 8.9 W, and the exergy recovered during the discharging process varied between 2.1 W and 3.4 W.

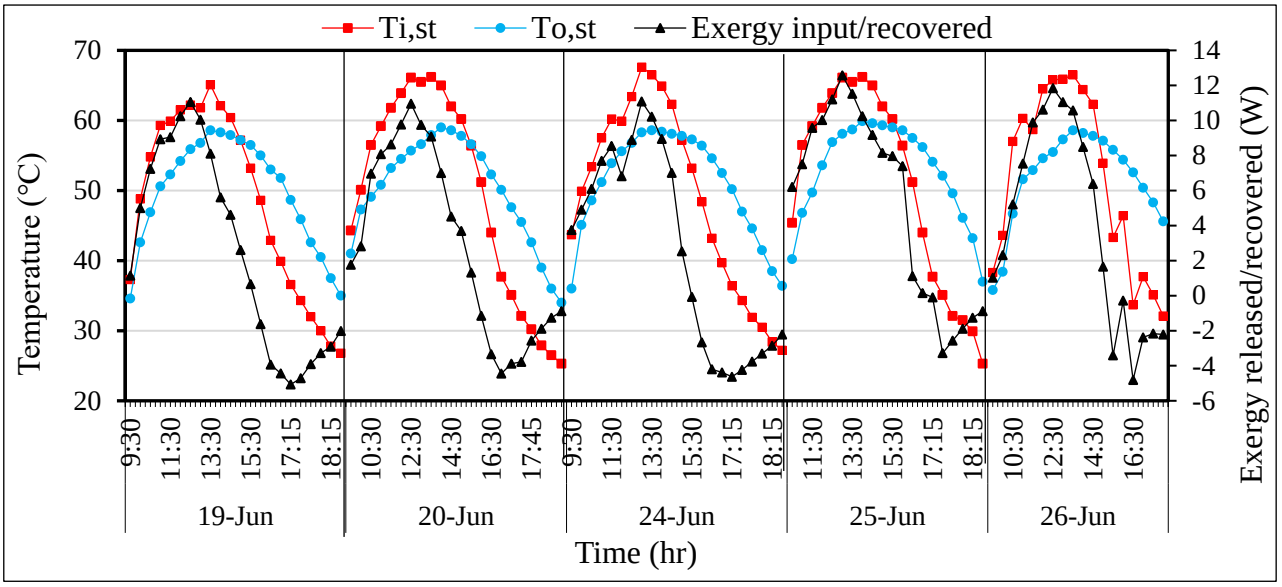

Figure 7. Exergy input/recovered by the air during the charging and discharging process.

3.6. Temperature variations of the paraffin wax

Figure 8 (a) shows the temperature variations of the paraffin wax at different locations of the energy storage during the charging and discharging processes. Apart from measuring the inlet and outlet temperatures of the heat transfer fluid, measuring the temperatures of the wax at different locations gives the best information about the melting and freezing behavior of the wax. Three thermocouples were fixed near the inlet (T_{c8}), at the centre (T_{c9}) and near the outlet (T_{c10}) of the energy storage. It is observed that, near the inlet of the energy storage, the temperature of the wax increased and decreased first. The temperature of the wax increased as the inlet air temperature of the storage increased and decreased when the inlet air temperature became lower than that of the PCM. The PCM is said to be completely melted when its temperature at the three locations reaches the melting temperature of the PCM and does not change. The average temperature variation of the wax is also shown in Figure 8 (b).

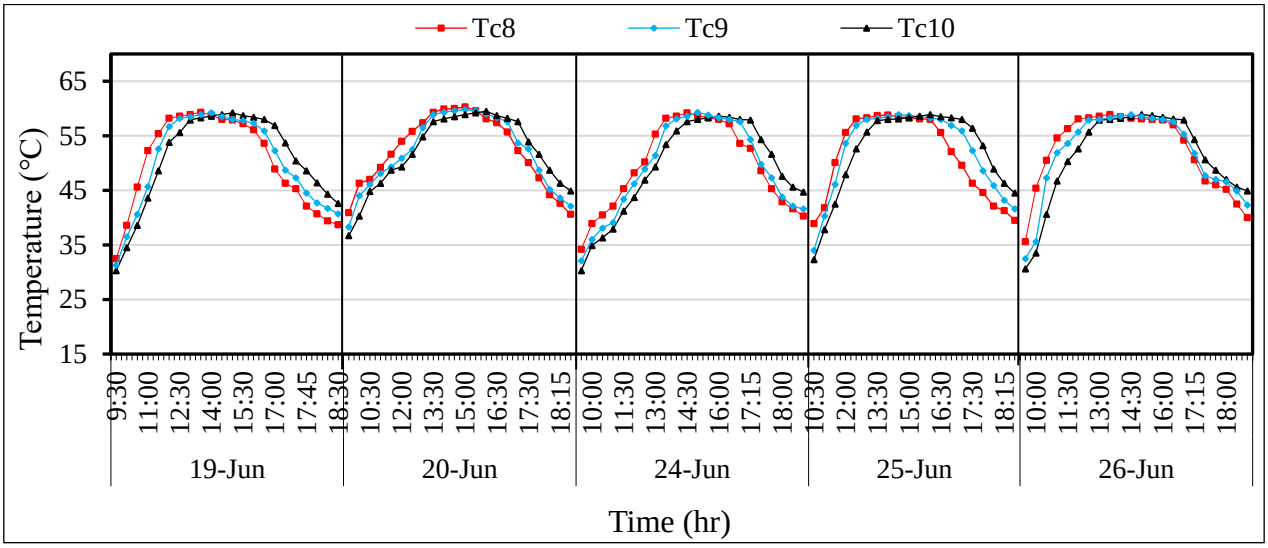

(a)

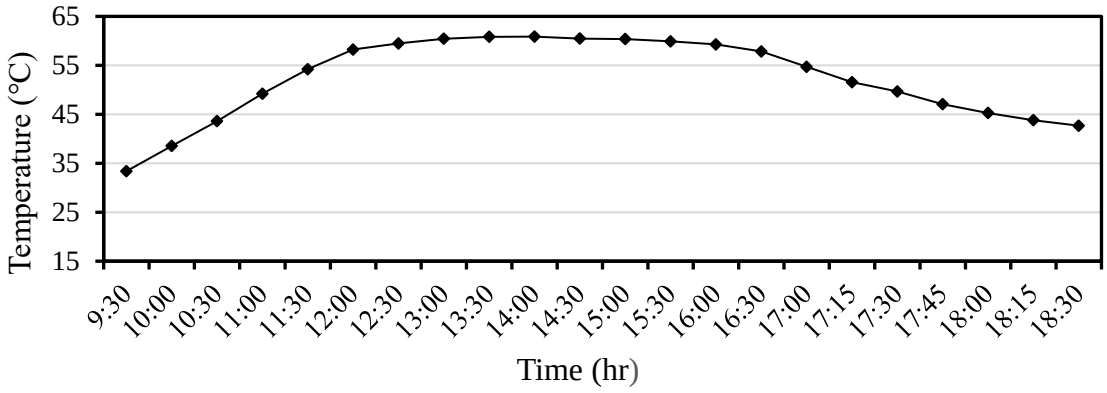

(b)

Figure 8. (a) Variation of wax temperature at different locations and (b) average temperature variation of the wax.

3.7. Variation of heat used by the drying chamber with inlet and outlet temperatures

The temperature variations of the drying air at the inlet and outlet of the drying chamber for the three consecutive days of drying is depicted in Figure 9. The inlet temperature of the drying chamber varied between 40 ℃ and 57 ℃, whereas the outlet temperature varied between 35 ℃ and 47 ℃. The outlet air temperature of the drying chamber increased with the number of days of drying due to the decreased moisture content of the fish. During the first day of drying, the drying air takes more moisture than during the latter days, resulting in a lower outlet temperature during the first day. The maximum heat used in the drying chamber varied between 10 W and 145 W. The heat used increased as the inlet temperature of the drying chamber increased and decreased as it decreased. It is also observed that the heat used during the first day was higher, and it decreased as the drying time increased, since the amount of moisture removed is lower toward the end of drying compared to the early days, resulting in a higher outlet air temperature of the drying chamber.

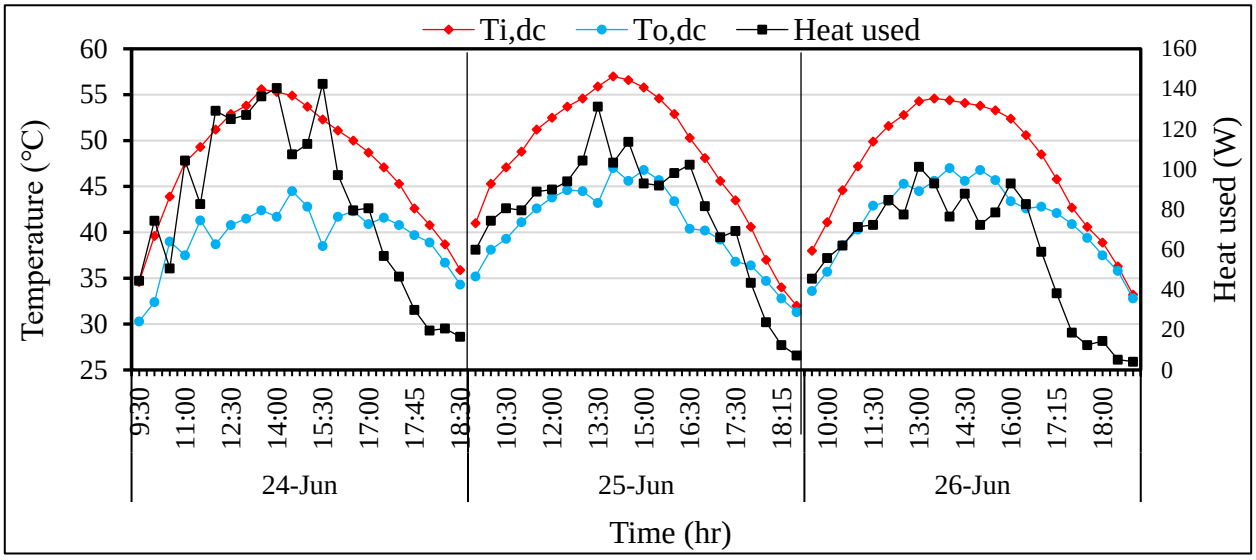

Figure 9. Variation of heat used by the drying chamber with inlet and outlet temperatures.

3.8. Efficiency of the drying chamber

Figure 10 shows the variation of thermal efficiency of the drying chamber with time. The thermal efficiency of the drying chamber varied from 13% to 62% during the three consecutive days of drying, and the average thermal efficiency of the drying chamber was 35.4%. It is observed that the thermal efficiency of the drying chamber decreased as the drying time advanced, and it was higher for the first day and decreased with the next days. This is due to the high amount of moisture removed during the first day of drying, resulting in a high temperature drop between the inlet and outlet of the drying chamber. The thermal efficiency of the drying chamber also decreased during the last hours of drying in each day, as the inlet temperature of the drying chamber decreased during the last hours.

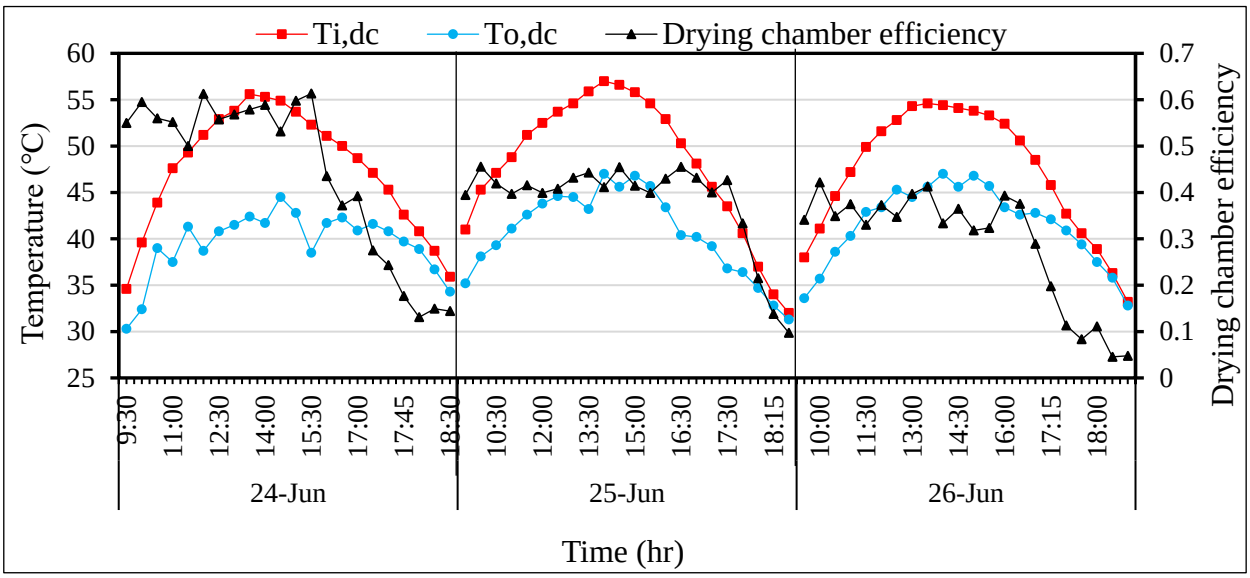

Figure 10. Variation of drying chamber efficiency.

3.9. Variations of exergy inflow, outflow and efficiency of the drying chamber

Figure 11 shows the variations of exergy inflow, exergy outflow and exergy efficiency of the drying chamber. The exergy inflow depends on the inlet temperature of the drying chamber, whereas the exergy outflow is related to the outlet temperature variation of the drying chamber. The exergy efficiency of the drying chamber varied between 15.4% and 90.8%, and the average exergetic efficiency was 52.2%. The exergy efficiency of the drying chamber was higher for the last day of drying than for the first two days, as the amount of moisture left in the fish was lower, resulting in a higher exergy outflow due to the increase in outlet temperature of the chamber. During the last hours of drying, the inlet temperature of the drying chamber decreased, resulting a lower exergy inflow. However, the outlet temperature of the drying chamber does not decrease in the same manner as the inlet temperature due to the accumulated heat released from the chamber to the air, resulting in an addition of exergy. Therefore, the exergy efficiency was higher during the last hours of drying each day. Similar trends of exergy efficiencies were reported by [37] and [42].

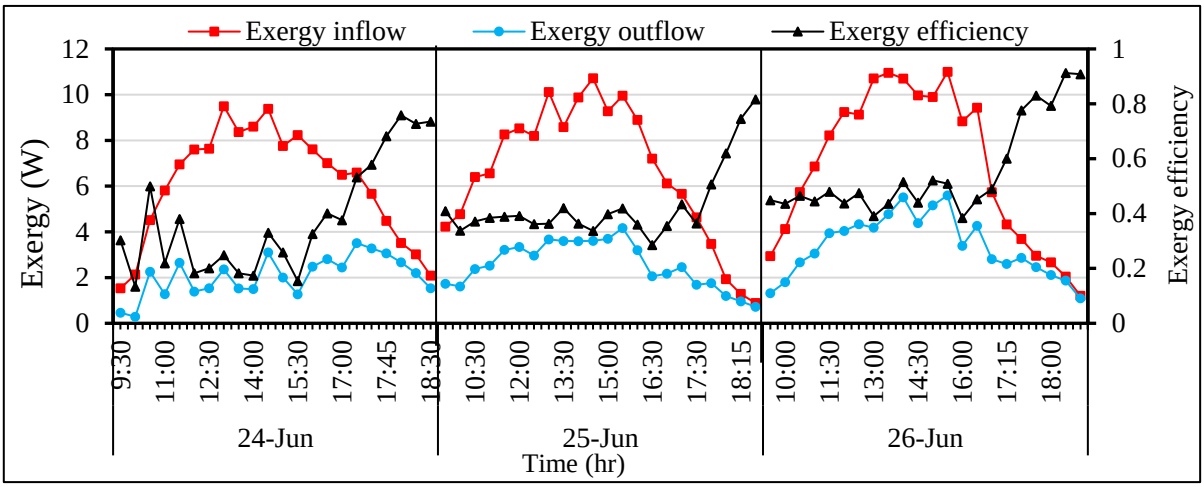

Figure 11. Variations of exergy inflow, exergy outflow and exergy efficiency of the drying chamber.

3.10. Performance of the drying system

The variation of moisture content with drying time for the three consecutive days of drying is shown in Figure 12. The moisture content of the fish is determined by measuring the weight of the fish and calculating the weight loss in a three-hour interval. The moisture content of the fish was reduced from the initial value of 75% (w.b.) to a final moisture content of 12.5% (w.b.) in 21 hrs. The moisture content of the fish was reduced from 75% (w.b.) to 45% (w.b.), 24% (w.b.) and 12.5% (w.b.) during the first, second and third days of dryin,g respectively. Similar results of drying time by drying products with an indirect mode solar dryer integrated with PCM were reported by [13] and [17]. Figure 13 (a) shows a photograph of fresh fish samples taken before they were loaded into the drying chamber, and (b) shows a photograph taken after drying in the solar dryer. It is clearly observed from Figure 13 that the colour and texture of the fish were preserved during the drying process.

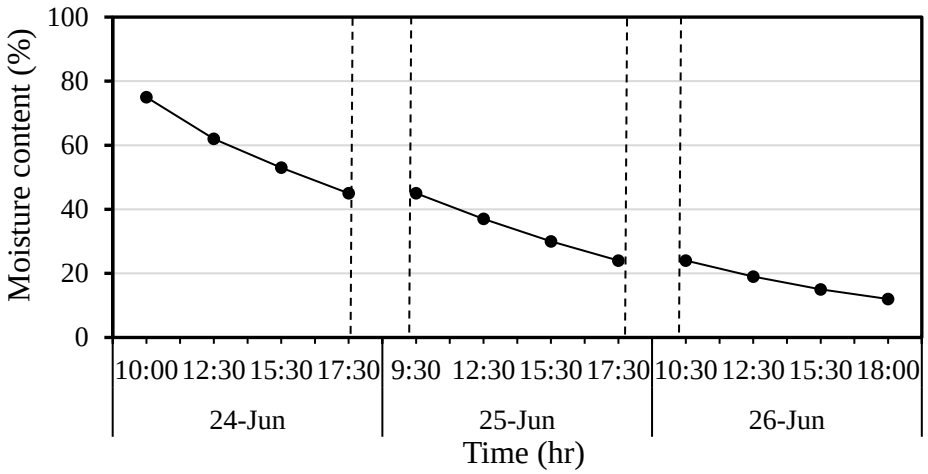

Figure 12. Variation of moisture content of the fish with drying time.

(a) (b)

Figure 13. Fish samples (a) before drying and (b) after drying.

Overall, 3.57 kg of moisture was evaporated from 5 kg of fresh fish, reducing the moisture content of the fish from an initial value of 75.1% (w.b.) to a final value of 12.5% (w.b.). The average solar radiation intensity falling on the surface of the solar air heater is estimated to be 539.6 W/m^2. The area of the solar air heater was 2.06 m^2, and the power consumed by the blower was 100 W. The dryer was operated for 7 hrs per day. The latent heat of evaporation of water at an average drying air temperature of 50 ℃ is 2396.5 kJ/kg, and the heat required to evaporate 3.57 kg of moisture from the fish was 8.4 MJ. The total energy input to the drying system was determined from Eq (22) and found to be 91.6 MJ. The specific energy consumption of the dryer was determined from Eq (21) and was found to be 7.3 kWh per kg of moisture. From the 7.3 kWh per kilogram of moisture consumption, the electrical energy consumption of the blower per kilogram of moisture removal was 0.6 kWh, which is 8.3% of the total specific energy consumption of the dryer. The remaining 91.7% of energy

consumed by the dryer was harvested from a free, easily available, eco-friendly, renewable type of energy, solar energy. References [41] and [43] reported similar results of specific energy consumption of solar dryers. The overall efficiency of the drying system was determined using Eq (23) and found to be 9.4%. References [7,9,17,44] reported similar results for drying fish, ginger and coconuts, respectively.

4. Conclusions

This study presented an experimental investigation of a solar dryer integrated with a shell and tube type LHS system with paraffin wax as a PCM for drying fish. The PCM was placed separately between the SAH and the drying chamber to reduce the possible heat losses to the sides of the SAH and the drying chamber when it is placed inside these components. Energy and exergy analysis was used to evaluate the performance of the dryer, and the following conclusions are drawn from the study.

- The outlet temperature of the SAH increased with increasing solar radiation intensity. As the solar radiation intensity increased, the amount of heat absorbed by the SAH increased. The temperature of the absorber plate increased, and this in turn increased the temperature of the air passing through the SAH. The energy and exergy efficiencies of the SAH also increased with increasing solar radiation intensity, and the average energy and exergy efficiencies of the double pass SAH were 25% and 1.5%, respectively.
- Integration of the energy storage reduced the fluctuations in the outlet air temperature of the SAH and extended the drying process beyond the sunny hours. The average energy and exergy efficiencies of the energy storage varied from 38.7% to 45% and 13.6% to 17.5%, respectively.
- The average energy and exergy efficiencies of the drying chamber were 35% and 52%, respectively. The specific energy consumption was 7.3 kWh per kilogram of moisture, and the electrical energy consumption of the blower was 0.6 kWh per kilogram of moisture, which was 8.3% of the total energy consumption. The remaining 91.7% of energy was harvested from solar energy. Overall, 3.57 kg moisture was removed from 5 kg of fresh fish while drying the fish from an initial moisture content of 75% (w.b.) to a final moisture content of 12.5% (w.b.) within 21 hrs of drying. This method preserved the color and texture of the product, and the overall efficiency of the drying system was 9.4%.

Acknowledgments

This research is funded by Adama Science and Technology University under the grant number ASTU/SM-R/143/19, Adama, Ethiopia.

Conflict of interest

The authors declare no conflict of interest.

References

1. Tesfamichael A (2004) Experimental analysis for performance evaluation of solar dryer. *Department of Mechanical Engineering, AAU*. Available from: https://manualzz.com/doc/7178691.
2. Gram L, Dalgaard P (2002) Fish spoilage bacteria-problems and solutions. *Curr Opin Biotechnol* 13: 262–266. https://doi.org/10.1016/S0958-1669(02)00309-9
3. Tesfay S, Teferi M (2017) Assessment of fish post-harvest losses in Tekeze dam and Lake Hashenge fishery associations: northern Ethiopia. *Agric Food Secur* 6: 4. https://doi.org/10.1186/s40066-016-0081-5
4. Kituu GM, Shitanda D, Kanali CL, et al. (2010) Thin layer drying model for simulating the drying of Tilapia fish (Oreochromis niloticus) in a solar tunnel dryer. *J Food Eng* 98: 325–331. https://doi.org/10.1016/j.jfoodeng.2010.01.009
5. Swami VM, Autee AT, Anil TR (2018) Experimental analysis of solar fish dryer using phase change material. *J Energy Storage* 20: 310–315. https://doi.org/10.1016/j.est.2018.09.016
6. Asmare E, Tewabe D, Mohamed B, et al. (2015) Pre-Scaling up of solar tent fish drier in northern and north western part of lake tana, Ethiopia. *Int J Aquacult Fish Sci* 1: 48–53. https://doi.org/10.17352/2455-8400.000009
7. Hubackova A, Kucerova I, Chrun R, et al. (2014) Development of solar drying model for selected Cambodian fish species. *Sci World J*, 2014. https://doi.org/10.1155/2014/439431
8. Ayyappan S, Mayilsamy K (2012) Solar tunnel drier with thermal storage for drying of copra. *Int J Energy Technol Policy* 8: 3–13. https://doi.org/10.1504/IJETP.2012.046017
9. Ayyappan S, Mayilsamy K, Sreenarayanan VV (2016) Performance improvement studies in a solar greenhouse drier using sensible heat storage materials. *Heat Mass Transfer* 52: 459–467. https://doi.org/10.1007/s00231-015-1568-5
10. Aissa W, El-Sallak M, Elhakem A (2012) An experimental investigation of forced convection flat plate solar air heater with storage material. *Therm Sci* 16. https://doi.org/10.2298/TSCI110607006A
11. Shalaby SM, Bek MA, El-Sebaii AA (2014) Solar dryers with PCM as energy storage medium: A review. *Renewable Sustainable Energy Rev* 33: 110–116. https://doi.org/10.1016/j.rser.2014.01.073
12. Bal LM, Satya S, Naik SN, et al. (2011) Review of solar dryers with latent heat storage systems for agricultural products. *Renewable Sustainable Energy Rev* 15: 876–880. https://doi.org/10.1016/j.rser.2010.09.006
13. Shalaby SM, Bek MA (2014) Experimental investigation of a novel indirect solar dryer implementing PCM as energy storage medium. *Energy Convers Manage* 83: 1–8. https://doi.org/10.1016/j.enconman.2014.03.043
14. Reyes A, Mahn A, V ásquez F (2014) Mushrooms dehydration in a hybrid-solar dryer, using a phase change material. *Energy Convers Manage* 83: 241–248. https://doi.org/10.1016/j.enconman.2014.03.077
15. Jain D, Tewari P (2015) Performance of indirect through pass natural convective solar crop dryer with phase change thermal energy storage. *Renewable Energy* 80: 244–250. https://doi.org/10.1016/j.renene.2015.02.012

16. Shringi V, Kothari S, Panwar NL (2014) Experimental investigation of drying of garlic clove in solar dryer using phase change material as energy storage. *J Therm Anal Calorim* 118: 533–539. https://doi.org/10.1007/s10973-014-3991-0
17. Sain P, Songara V, Karir R, et al. (2013) Natural convection type solar dryer with latent heat storage. *2013 International Conference on Renewable Energy and Sustainable Energy (ICRESE)*, 9–14. https://doi.org/10.1109/ICRESE.2013.6927808
18. Zachariah R, Maatallah T, Modi A (2021) Environmental and economic analysis of a photovoltaic assisted mixed mode solar dryer with thermal energy storage and exhaust air recirculation. *Int J Energy Res* 45: 1879–1891. https://doi.org/10.1002/er.5868
19. Azaizia Z, Kooli S, Hamdi I, et al. (2020) Experimental study of a new mixed mode solar greenhouse drying system with and without thermal energy storage for pepper. *Renewable Energy* 145: 1972–1984. https://doi.org/10.1016/j.renene.2019.07.055
20. Singh D, Mall P (2020) Experimental investigation of thermal performance of indirect mode solar dryer with phase change material for banana slices. *Energy Sources, Part A: Recovery, Util, Environ Effects*, 1–18. https://doi.org/10.1080/15567036.2020.1810825
21. Vijayrakesh K, Muthuvel S, Gopinath GR, et al. (2021) Experimental investigation of the performance of paraffin wax-packed floor on a solar dryer. *J Energy Storage* 43: 103163. https://doi.org/10.1016/j.est.2021.103163
22. Abi Mathew A, Thangavel V (2021) A novel thermal energy storage integrated evacuated tube heat pipe solar dryer for agricultural products: Performance and economic evaluation. *Renewable Energy* 179: 1674–1693. https://doi.org/10.1016/j.renene.2021.07.029
23. Kondareddy R, Sivakumaran N, Radha Krishnan K, et al. (2021) Performance evaluation and economic analysis of modified solar dryer with thermal energy storage for drying of blood fruit (Haematocarpus validus). *J Food Process Preserv* 45: e15653. https://doi.org/10.1111/jfpp.15653
24. Sözen A, Kazancıoğlu FŞ, Tuncer AD, et al. (2021) Thermal performance improvement of an indirect solar dryer with tube-type absorber packed with aluminum wool. *Sol Energy* 217: 328–341. https://doi.org/10.1016/j.solener.2021.02.029
25. Selimefendigil F, Şirin C, Öztop HF (2022) Improving the performance of an active greenhouse dryer by integrating a solar absorber north wall coated with graphene nanoplatelet-embedded black paint. *Sol Energy* 231: 140–148. https://doi.org/10.1016/j.solener.2021.10.082
26. Çiftçi E, Khanlari A, Sözen A, et al. (2021) Energy and exergy analysis of a photovoltaic thermal (PVT) system used in solar dryer: A numerical and experimental investigation. *Renewable Energy* 180: 410–423. https://doi.org/10.1016/j.renene.2021.08.081
27. Khanlari A, Sözen A, Afshari F, et al. (2021) Energy-exergy and sustainability analysis of a PV-driven quadruple-flow solar drying system. *Renewable Energy* 175: 1151–1166. https://doi.org/10.1016/j.renene.2021.05.062
28. Seddegh S, Wang X, Henderson AD (2016) A comparative study of thermal behaviour of a horizontal and vertical shell-and-tube energy storage using phase change materials. *Appl Therm Eng* 93: 348–358. https://doi.org/10.1016/j.applthermaleng.2015.09.107
29. Gunjo DG, Jena SR, Mahanta P, et al. (2018) Melting enhancement of a latent heat storage with dispersed Cu, CuO and Al_2O_3 nanoparticles for solar thermal application. *Renewable Energy* 121: 652–665. https://doi.org/10.1016/j.renene.2018.01.013
30. Vyshak NR, Jilani G (2007) Numerical analysis of latent heat thermal energy storage system. *Energy Convers Manage* 48: 2161–2168. https://doi.org/10.1016/j.enconman.2006.12.013

31. Lingayat AB, Suple YR (2013) Review on phase change material as thermal energy storage medium: materials, application. *Int J Eng Res Appl* 3: 916–921.
32. Cengel YA, Boles MA (2007) *Thermodynamics: An Engineering Approach 6th Edition (SI Units)*. The McGraw-Hill Companies, Inc., New York. Available from: https://www.amazon.com/Thermodynamics-Engineering-Approach-Cengel-2007-05-22/dp/B01FIXO1W6.
33. Ramani BM, Gupta A, Kumar R (2010) Performance of a double pass solar air collector. *Sol Energy* 84: 1929–1937. https://doi.org/10.1016/j.solener.2010.07.007
34. Struckmann F (2008) Analysis of a flat-plate solar collector. *Heat and Mass Transport, Project Report, 2008MVK160*. Available from: https://scholar.google.com/scholar?hl=en&as_sdt=0%2C5&q=34.%09Struckmann+F+%282008%29+Analysis+of+a+flat-plate+solar+collector.+Heat+and+Mass+Transport%2C+Project+Report%2C+2008MVK160&btnG=.
35. Dincer I, Rosen MA (2007) Energetic, exergetic, environmental and sustainability aspects of thermal energy storage systems. *Therm Energy Storage Sustainable Energy Consumption*, 23–46. https://doi.org/10.1007/978-1-4020-5290-3_2
36. Akbulut A, Durmuş A (2010) Energy and exergy analyses of thin layer drying of mulberry in a forced solar dryer. *Energy* 35: 1754–1763. https://doi.org/10.1016/j.energy.2009.12.028
37. Fudholi A, Sopian K, Yazdi MH, et al. (2014) Performance analysis of solar drying system for red chili. *Sol Energy* 99: 47–54. https://doi.org/10.1016/j.solener.2013.10.019
38. Jafarkazemi F, Ahmadifard E (2013) Energetic and exergetic evaluation of flat plate solar collectors. *Renewable Energy* 56: 55–63. https://doi.org/10.1016/j.renene.2012.10.031
39. Omojaro AP, Aldabbagh LBY (2010) Experimental performance of single and double pass solar air heater with fins and steel wire mesh as absorber. *Appl Energy* 87: 3759–3765. https://doi.org/10.1016/j.apenergy.2010.06.020
40. El-Khawajah MF, Aldabbagh LBY, Egelioglu F (2011) The effect of using transverse fins on a double pass flow solar air heater using wire mesh as an absorber. *Sol Energy* 85: 1479–1487. https://doi.org/10.1016/j.solener.2011.04.004
41. Abdelkader TK, Salem AE, Zhang Y, et al. (2021) Energy and exergy analysis of carbon nanotubes-based solar dryer. *J Energy Storage* 39: 102623. https://doi.org/10.1016/j.est.2021.102623
42. Akpinar EK (2010) Drying of mint leaves in a solar dryer and under open sun: modelling, performance analyses. *Energy Convers Manage* 51: 2407–2418. https://doi.org/10.1016/j.enconman.2010.05.005
43. Ndukwu MC, Onyenwigwe D, Abam FI, et al. (2020) Development of a low-cost wind-powered active solar dryer integrated with glycerol as thermal storage. *Renewable Energy* 154: 553–568. https://doi.org/10.1016/j.renene.2020.03.016
44. Sengar SH, Khandetod YP, Mohod AG (2009) Low cost solar dryer for fish. *African J Environ Sci Technol* 3. https://www.ajol.info/index.php/ajest/article/view/46076